The Flinders University of South Australia

INSTITUTE FOR ATOMIC STUDIES

SCHOOL OF PHYSICAL SCIENCES

ISSN 0725-785X

"IONISATION OF ATOMIC HYDROGEN AT INTERMEDIATE MOMENTUM TRANSFER"

I.E. McCarthy, E. Weigold, X. Zhang and Y. Zheng

August, 1988

IONISATION OF ATOMIC HYDROGEN AT INTERMEDIATE MOMENTUM TRANSFER

I.E. McCarthy, E. Weigold, X. Zhang* and Y. Zheng

Institute for Atomic Studies, The Flinders University of South Australia, Bedford Park, S.A. 5042, Australia.

ABSTRACT

Relative differential cross sections for the asymmetric coplanar (e,2e) reaction have been measured in three energy-sharing regions, for two of which the ionisation peak is about 1 a.u. off the Bethe ridge. Momentum transfer is intermediate between large (binary) and small (dipole) values, where the distorted-wave impulse and second Born approximations respectively give a good account of the experimental data. In addition to these approximations the distorted-wave Born approximation is calculated. It is somewhat superior to the distorted-wave impulse approximation and very much better than the second Born approximation.

PACS classification 34.80.Dp

1. INTRODUCTION

In studying the mechanism of the ionisation of atoms by electron impact atomic hydrogen is the ideal target because there is no question about whether we can describe the target ground state with sufficient accuracy. Since there is no closed-form three-body theory for Coulomb potentials, understanding is achieved by an iterative interaction of experiment and theory by which it is hoped to find a good description of the reaction in a broad kinematic region.

Ionisation has been studied mainly in two broad kinematic regions, characterised by high and low momentum transfer. The description of the reaction has turned out to emphasise quite different aspects of the three-body system in the two regions. For low momentum transfer the incident electron undergoes rather a long-range interaction with the target, influenced significantly by the potentials of the active target electron and of the residual ion. Ionisation is described quite well by the second Born approximation or improved descriptions based on the Born series (Joachain and Pireaux 1986, Sharma and Srivastava 1987) in which both potentials, called v and V respectively, are treated roughly on an equal basis, the Born series being summed to second order in both. High momentum transfer results from a close electron-electron collision. The plane-wave impulse approximation (PWIA) treats only the interaction v, but sums the corresponding Born series to all orders, giving the electron-electron t-matrix t. The distorted-wave impulse approximation (DWIA) treats the interactions of the fast electrons with the rest of the system also in all orders in the appropriate two-body problems by using the corresponding elastic scattering functions (distorted waves). However it is necessary for computation to make a factorisation approximation in which the t-matrix and the distorted waves contribute to separate factors. The factorisation is exact only in the PWIA. Noncoplanar symmetric ionisation is described essentially within experimental error for many targets by the DWIA (McCarthy and Weigold 1988), as is coplanar ionisation for recoil momentum near zero, i.e. near the Bethe ridge (Lahmam-Bennani *et al* 1988).

Absolute experimental cross sections are available in both high- and low-momentum-transfer regions. For low momentum transfer several normalisation methods involving known low-momentum limits agree (Lahmam-Bennani *et al* 1987). For high momentum transfer absolute cross sections have been directly measured (Beaty *et al* 1977, Stefani *et al* 1978, van Wingerden *et al* 1979, 1981).

The present experiments are done at a total energy of 400eV. The momenta of the incident $\mathbf{k}_0$, fast $\mathbf{k}_A$ and slow $\mathbf{k}_B$ electrons are coplanar. The scattering angle of the fast electron θ_A is fixed at 30°. Three energy-sharing regions are studied in which the slow electron has energy 50, 100 and 200eV. In each region the relative differential cross section is measured as a function of the polar angle θ_B of the slow electron. The relative normalisation of the three energy regions is not measured. Theoretical descriptions are tested only by the shape of the θ_B profile in each energy region. The recoil momentum at the peak for the three regions is 0.87, 0.09 and -0.95 a.u. respectively. The first and third regions are well off the Bethe ridge.

Three approximations are compared with the experimental data. In addition to the second Born approximation and the DWIA we calculate the distorted-wave Born approximation (DWBA). This obtains very accurate total ionisation cross sections at energies above about ten times the ionisation threshold for many atoms and ions (Younger 1981 and references therein).

There is an important theoretical reason for testing the DWBA. It is the most detailed approximation that is computationally feasible for the effect of the continuum in an ab initio optical potential for scattering (McCarthy and Stelbovics 1980).

2. Experimental Details

The coplanar asymmetric apparatus used in these measurements has been described in detail by Weigold *et al* (1979) and Lohmann *et al* (1984). The only difference was that one of the cylindrical mirror analysers was replaced by a hemispherical one with five element retarding lens. A 1mm × 1mm slit was placed in the centre of the exit plate of the hemispherical analyser, and the transmitted electrons were detected using channel electron multipliers. The hemispherical and the cylindrical analysers, detecting the lower energy "ejected" and the higher energy "scattered" electrons respectively, could be independently rotated in the scattering plane about the interaction region by computer-controlled stepping motors. The pass energy through the analysers was kept fixed at 30eV and the energy calibration was performed using the Auger lines of argon with an incident energy of 860eV. Collimation of the electron beam ensured that the angular divergence of the beam was less than 1°. Standard coincidence signal processing was used.

A pyrex RF discharge tube was used to dissociate the molecular hydrogen. Typical operating conditions were RF frequencies in the range 35-45MHz and power levels of the order of 20-30 watts. The degree of dissociation was measured in a coplanar symmetric (e,2e) experiment at a total energy in the exit channel of 400eV as described by Lower *et al* (1987). The dissociation ratio is given by

$$\eta = \frac{1}{1 + \sqrt{2}\,(\frac{\sigma_1}{\sigma_2})(\frac{S_2}{S_1})},$$

where σ_1 and σ_2 denote the triple differential cross sections for atomic and molecular hydrogen respectively, and S_1 and S_2 the measured signals under the peaks centred at separation energies of 13.6eV and 15.9eV respectively. The factor of $\sqrt{2}$ corrects for the difference in atomic and molecular velocities. The dissociation was typically 70%, using the plane wave impulse approximation value of 1.24 for the ratio σ_2/σ_1 for $\xi = 45°$ and 200eV outgoing electrons.

Care was taken to align the interaction region with the centre of rotation of the two

analysers. A skimmer was used to confine the atomic beam to be within the viewing angles of the analysers. The zero angle and angular dependence of the detection efficiencies of the two analysers were checked by measuring the known cross section for elastic scattering from atomic hydrogen (van Wingerden *et al* 1977).

3. Theoretical approximations

The differential cross section for the (e,2e) reaction is

$$\frac{d^5\sigma}{d\hat{\mathbf{k}}_A d\hat{\mathbf{k}}_B dE_A} = (2\pi)^4 \frac{k_A k_B}{k_0} \Sigma_{av} \mid T(\mathbf{k}_A, \mathbf{k}_B, \mathbf{k}_0) \mid^2, \tag{1}$$

where Σ_{av} denotes an average over initial and sum over final spin degeneracies. We consider three different approximations to the three-body T-matrix T.

The distorted-wave approximations are based on considering the primary electron-electron collision inside the atom as being governed by the free electron-electron collision operator t. The wave functions representing the interaction of the fast electrons with the target are elastic scattering functions calculated in the appropriate potential. This is the static potential of the atom for the incident electron, and the static potential of the ion (the Coulomb potential for hydrogen) for the slow outgoing electron. A better approximation would be to include exchange and higher-order potentials representing the effects of unobserved channels, but their effects have never been observable (McCarthy and Weigold 1988).

For the fast outgoing electron the first approximation to the potential is not obvious. It could be the ion potential or it could be the ion potential screened in some way by the slow electron, the extreme being the target potential. We consider the two extremes, ion and target potentials.

The basic approximation is

$$T(\mathbf{k}_A, \mathbf{k}_B, \mathbf{k}_0) = \langle \chi^{(-)}(\mathbf{k}_A) \chi^{(-)}(\mathbf{k}_B) \mid t \mid \psi_0 \chi^{(+)}(\mathbf{k}_0) \rangle. \tag{2}$$

Here ψ_0 represents the target ground state and

$$t = [1 + (-1)^S P_r] t_C, \tag{3}$$

where S is the total spin of the colliding electrons, P_r is the space-exchange operator and t_C is the Coulomb t-matrix (Chen and Chen 1972, McCarthy and Roberts 1987).

Since t is a nonlocal operator (2) involves a nine-dimensional integral which has proved too difficult to calculate. We make two alternative approximations to circumvent this difficulty.

The distorted-wave impulse approximation (DWIA) recognises that if the electron-target potentials are ignored for the fast electrons and $\chi^{(+)}(\mathbf{k})$ are plane waves then (2) factorises into a factor describing the electron-electron collision and a factor describing the target-ion structure. The approximation retains the factorisation and puts the distortion back into the structure factor.

$$T_{DWI}(\mathbf{k}_A, \mathbf{k}_B, \mathbf{k}_0) = \langle \mathbf{k}' \mid t \mid \mathbf{k} \rangle \langle \chi^{(-)}(\mathbf{k}_A)\chi^{(-)}(\mathbf{k}_B) \mid \psi_0 \chi^{(+)}(\mathbf{k}_0) \rangle. \tag{4}$$

where

$$\begin{aligned} \mathbf{k}' &= \tfrac{1}{2}(\mathbf{k}_A - \mathbf{k}_B), \\ \mathbf{k} &= \tfrac{1}{2}(\mathbf{k}_0 - \mathbf{q}), \\ \mathbf{q} &= \mathbf{k}_A + \mathbf{k}_B - \mathbf{k}_0. \end{aligned} \tag{5}$$

The distorted-wave Born approximation (DWBA) treats the electron-electron collision only in first order. It is not necessary now to factorise the integral (2) since v is a local operator and the integration is over six dimensions, for which computation is possible.

$$T_{DWB}(\mathbf{k}_A, \mathbf{k}_B, \mathbf{k}_0) = \langle \chi^{(-)}(\mathbf{k}_A)\chi^{(-)}(\mathbf{k}_B) \mid v \mid \psi_0 \chi^{(+)}(\mathbf{k}_0) \rangle. \tag{6}$$

The second Born approximation (BORN2) includes the potentials v and V up to second order.

$$T_{BORN2}(\mathbf{k}_A, \mathbf{k}_B, \mathbf{k}_0) = \langle \mathbf{k}_A \chi^{(-)}(\mathbf{k}_B) \mid v + (v+V)\frac{1}{E^{(+)} - H_T - K}(v+V) \mid \psi_0 \mathbf{k}_0 \rangle, \quad (7)$$

where H_T is the target Hamiltonian and K is the projectile kinetic energy operator. Exchange terms are omitted. The second-order tem is evaluated in the closure approximation (Byron *et al* 1980).

The DWBA gives excellent total ionisation cross sections for a wide range of atoms and ions at an energy above about ten times the ionisation threshold. The main contribution is from the very asymmetric region so that one would expect it to be a very good approximation in this region, where the second Born approximation is normally compared with experimental data. The DWBA describes the binary peak very well for helium (Müller-Fiedler *et al* 1985). In fig. 1 the DWBA and the second Born approximation are compared with the $e - H$ data of Ehrhardt *et al* (1985) at $E_0 = 250$eV, $E_B = 5$eV and $\theta_A = 3°$. These data have been put on an absolute scale in comparison with the optical oscillator strength by extrapolating the first Born approximation to zero momentum.

The DWBA is somewhat inferior to the second Born approximation in shape, since its binary peak is shifted to smaller angles than that of the experiment and the second Born approximation. Its magnitude is about 60% of the second Born and the theoretically-normalised data. This discrepancy is surprising in view of its success for total ionisation cross sections and helium differential cross sections. More information is needed on absolute cross sections in the very asymmetric kinematic region.

4. Results

The present experimental relative differential cross sections are given in table 1. They have been normalised at the maximum in each energy-sharing region to the DWBA.

The differential cross sections are compared with the three approximations in figs. 2-4. There is little to choose in shape between the DWBA and DWIA, although the DWBA is slightly better overall. There is a 2° shift of the DWIA peak to larger angles than the DWBA peak at $E_B = 200$eV. In absolute magnitude the DWIA peak is about 50% lower than the DWBA peak. BORN2 does not agree well in shape with the experimental data in any energy region. It is best in the most asymmetric region $E_B = 50$eV (fig. 2).

In each energy region the distorted-wave calculations use the unscreened ion in potential $Z_A = 1$ for the faster electron. Maximum screening is represented by using the target static potential for calculating $\chi^{(-)}(\mathbf{k}_A)$. The screening is expected to have maximum effect in the most asymmetric case $E_B = 50$eV. Fig. 5 shows that its effect is significant in the DWBA, producing a 4° shift to smaller θ_B. The shape of the screened DWBA near the peak is very similar to BORN2, but it is in worse agreement with experiment than the unscreened DWBA. A similar effect was found by Madison *et al* (1977).

5. Conclusions

The DWBA gives a satisfactory description of the shapes of 400eV differential cross section profiles for hydrogen in three coplanar ionisation regions. Two of these regions are about 1 a.u. off the Bethe ridge while the other peaks near the Bethe ridge. The DWIA gives a slightly poorer description for symmetric energies at $\theta_A = 30°$. The second Born approximation is unsatisfactory in all regions. The most satisfactory shape in the distorted-wave approximations is obtained by using the full ion potential for the faster electron. No significant effects of screening by the slower electron are detectable.

References

* Permanent address: Department of Modern Physics, The University of Science and Technology, Anhui, Hefei, China.

Beaty E C, Hesselbacher K H, Hong S P and Moore J H 1977 J.Phys.B:At.Mol.Phys. **10** 611

Byron F W Jr., Joachain C J and Pireaux B 1980 J.Phys.B:At.Mol.Phys. **13** L673

Chen J C Y and Chen A C 1972 Adv.At.Mol.Phys. **8** 71

Ehrhardt H, Knoth G, Schlemmer P and Jung K 1985 Phys.Lett. **110A** 92

Joachain C J and Pireaux B 1986 Comment.At.Mol.Phys. **17** 261

Lahmam-Bennani A, Avaldi L, Fainelli E and Stefani G 1988 J.Phys.B:At.Mol.Phys. **21**

Lahmam-Bennani A, Cherid M and Duguet A 1987 J.Phys.B:At.Mol.Phys. **20** 2531

Lohmann B, McCarthy I E, Stelbovics A T and Weigold E 1984 Phys.Rev.A **30** 758

Lower J, McCarthy I E and Weigold E 1987 J.Phys.B:At.Mol.Phys. **20** 4571

McCarthy I E and Roberts M J 1987 J.Phys.B:At.Mol.Phys. **20** L231

McCarthy I E and Stelbovics A T 1980 Phys.Rev.A **22** 502

McCarthy I E and Weigold E 1988 Rep.Prog.Phys. **51** 299

Madison D H, Calhoun R V and Shelton W N 1977 Phys.Rev.A **16** 552

Müller-Fiedler R, Schlemmer P, Jung K and Ehrhardt H 1985 Z.Phys.A **320** 89

Sharma S and Srivastava M K 1987 Phys.Rev.A **35** 1939

Stefani G, Camilloni R and Giardini-Guidoni A 1978 Phys.Lett. **64A** 364

Weigold E, Noble C J, Hood S T and Fuss I 1979 J.Phys.B:At.Mol.Phys. **12** 291

van Wingerden B, Kimman J T, van Tilburg M and deHeer F J 1981 J.Phys.B : At.Mol.Phys. **14** 2475

van Wingerden B, Kimman J T, van Tilburg M, Weigold E, Joachain C J, Pireaux B and deHeer F J 1979 J.Phys.B : At.Mol.Phys. **12** L627

van Wingerden B, Weigold E, deHeer F J and Nygaard K J 1977 J.Phys.B:At.Mol.Phys. **10** 1345

Table 1. Differential cross sections in the energy-sharing regions E_B = 50, 100 and 200eV. Relative experimental cross sections have been normalised at the maximum to the DWBA. Units are $10^{-3}a_0^2/(\mathrm{Sr}^2.\mathrm{Ryd})$. The total energy $E_A + E_B$ is 400eV and θ_A is 30°. Experimental errors in the final digits are shown in parentheses.

θ_B(deg.)	E_B=50eV	E_B=100eV	E_B=200eV
30	-	3 8(14)	0.50(16)
35	-0.2(4)	5.4(15)	0.88(20)
40	1.1(6)	4.6(15)	1.56(25)
45	0.5(5)	12.5(21)	2.32(29)
50	2.1(7)	28.4(29)	1.85(26)
55	4.7(10)	44.3(35)	1.51(23)
60	7.3(12)	53.7(39)	0.57(14)
65	7.2(12)	43.6(35)	0.11(8)
70	11.6(13)	22.6(26)	0.02(4)
75	9.0(12)	13.9(21)	0.03(4)
80	8.6(11)	7.0(15)	0.03(4)
85	3.8(8)	3.0(12)	-
90	2.0(6)	4.4(12)	-
95	0.8(4)	4.0(12)	-
100	1.2(4)	2.3(10)	-
105	1.2(4)	3.8(12)	-
110	0.1(2)	2.1(10)	-
115	0.4(3)	1.5(9)	-
120	0.2(2)	2.8(10)	-

Figure Captions

Fig. 1 Electron impact ionisation of hydrogen fo. $E_0 = 250$eV, $E_B = 5$eV, $\theta_A = 3°$. The experimental data and second Born calculation (broken curve) of Ehrhardt *et al* (1985) are compared with the present DWBA (full curve).

Fig. 2 Electron impact ionisation of hydrogen for $\theta_A = 30°$, $E_A = 350$eV, $E_B = 50$eV. The present experimental data are compared with DWBA (full curve), DWIA (long dashed curve) and BORN2 (short dashed curve). Atomic units here are $a_0^2/(\mathrm{Sr}^2\ \mathrm{Ryd})$.

Fig. 3 Electron impact ionisation of hydrogen for $\theta_A = 30°$, $E_A = 300$eV, $E_B = 100$eV. The present experimental data are compared with DWBA (full curve), DWIA (long dashed curve) and BORN2 (short dashed curve). Atomic units here are $a_0^2/(\mathrm{Sr}^2\ \mathrm{Ryd})$.

Fig. 4 Electron impact ionisation of hydrogen for $\theta_A = 30°$, $E_A = 200$eV, $E_B = 200$eV. The present experimental data are compared with DWBA (full curve), DWIA (long dashed curve) and BORN2 (short dashed curve). Atomic units here are $a_0^2/(\mathrm{Sr}^2\ \mathrm{Ryd})$.

Fig. 5 Comparison of the DWBA for $\theta_A = 30°$, $E_A = 350$eV, $E_B = 50$eV using the target potential (broken curve) and the ion potential (full curve) for the 350eV electron.

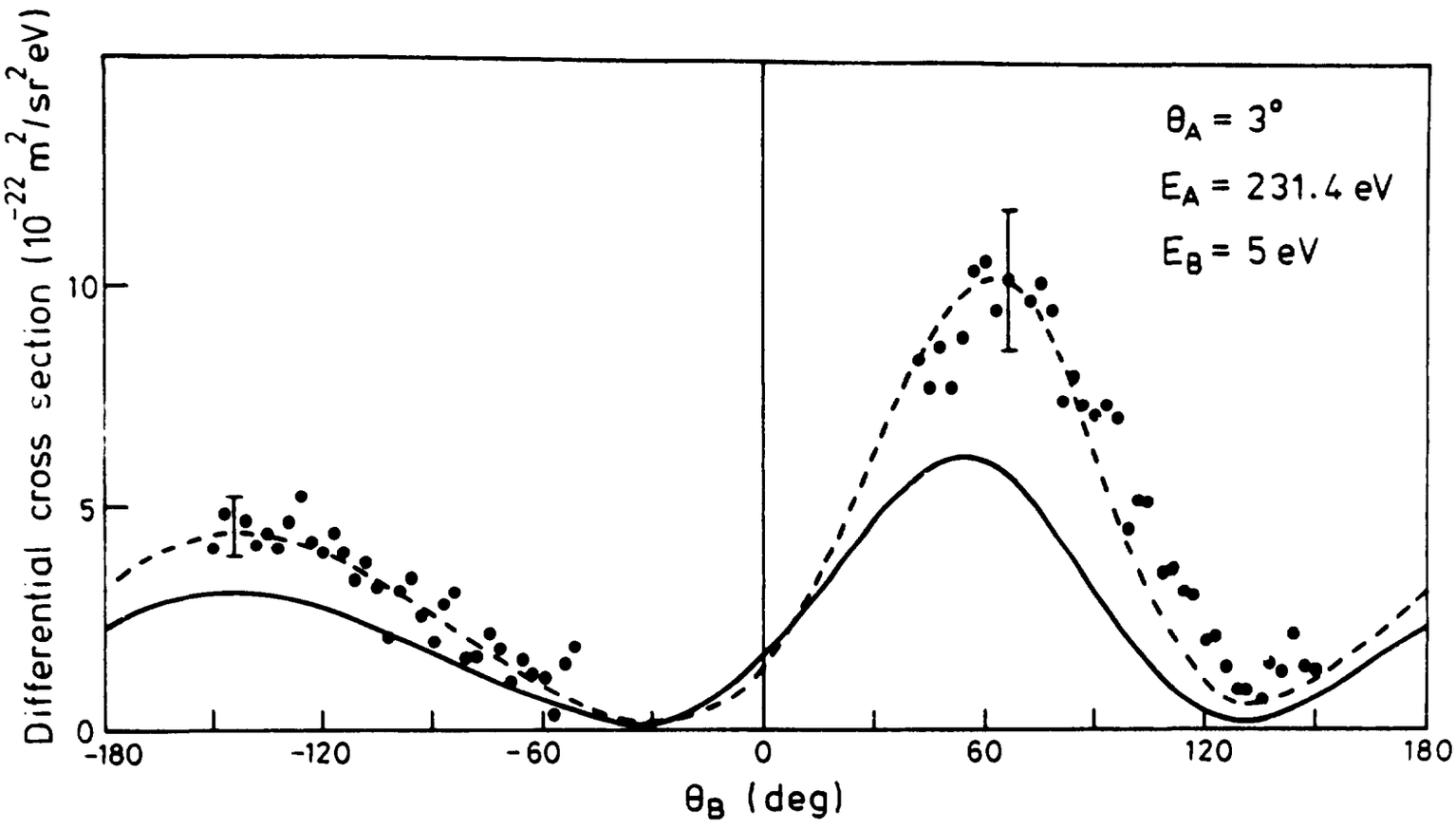
Differential cross section (10^{-22} m^2/sr^{2}eV)
θ_A = 3°
E_A = 231.4 eV
E_B = 5 eV
10
5
0
-180
-120
-60
0
60
120
180
θ_B (deg)

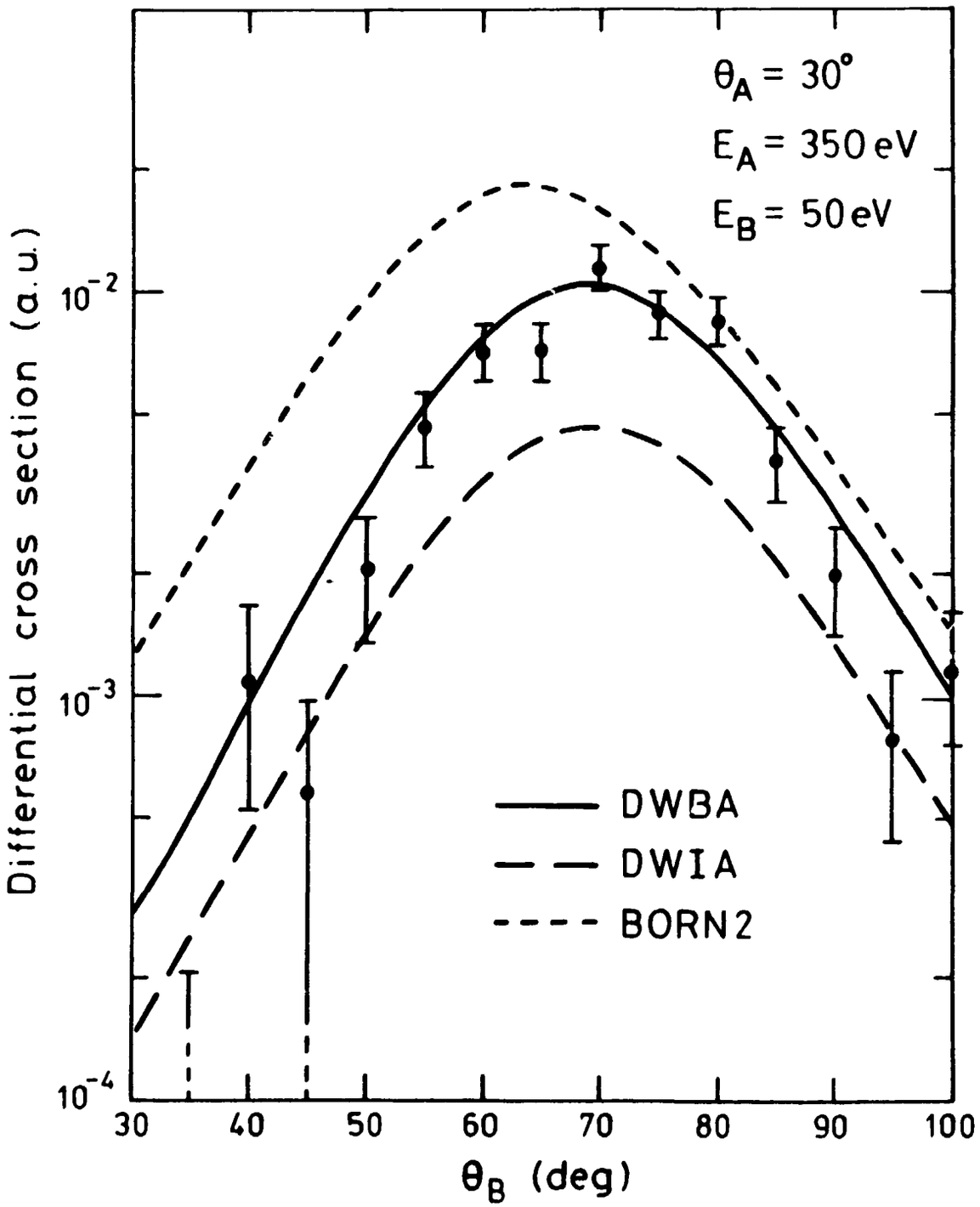
$\theta_A = 30°$
$E_A = 350\,eV$
$E_B = 50\,eV$
DWBA
DWIA
BORN2
Differential cross section (a.u.)
10^{-2}
10^{-3}
10^{-4}
30
40
50
60
70
80
90
100
θ_B (deg)

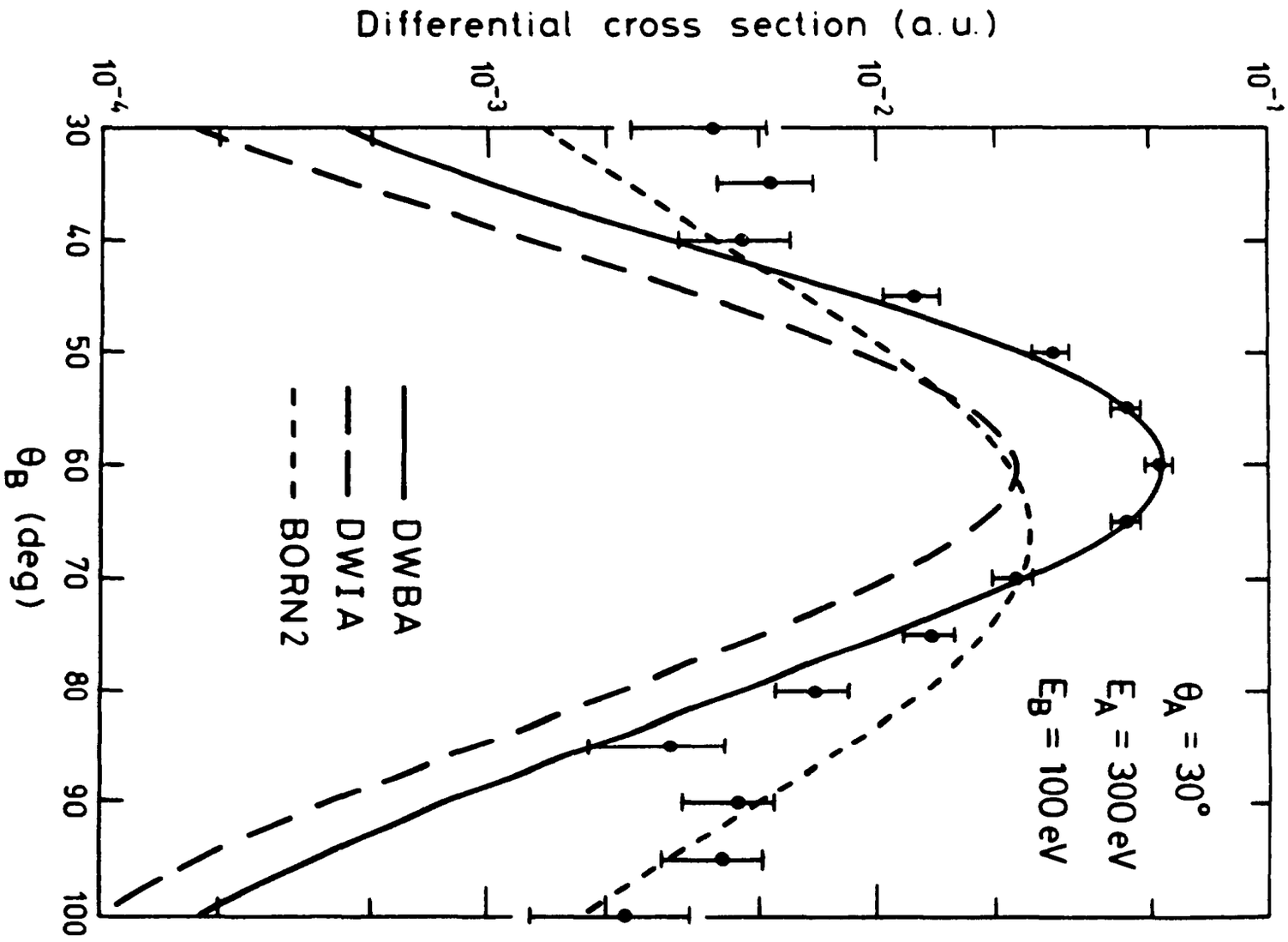
Differential cross section (a.u.)
10^{-4}
10^{-3}
10^{-2}
10^{-1}
30
40
50
60
70
80
90
100
θ_B (deg)
DWBA
DWIA
BORN2
$\theta_A = 30°$
$E_A = 300$ eV
$E_B = 100$ eV

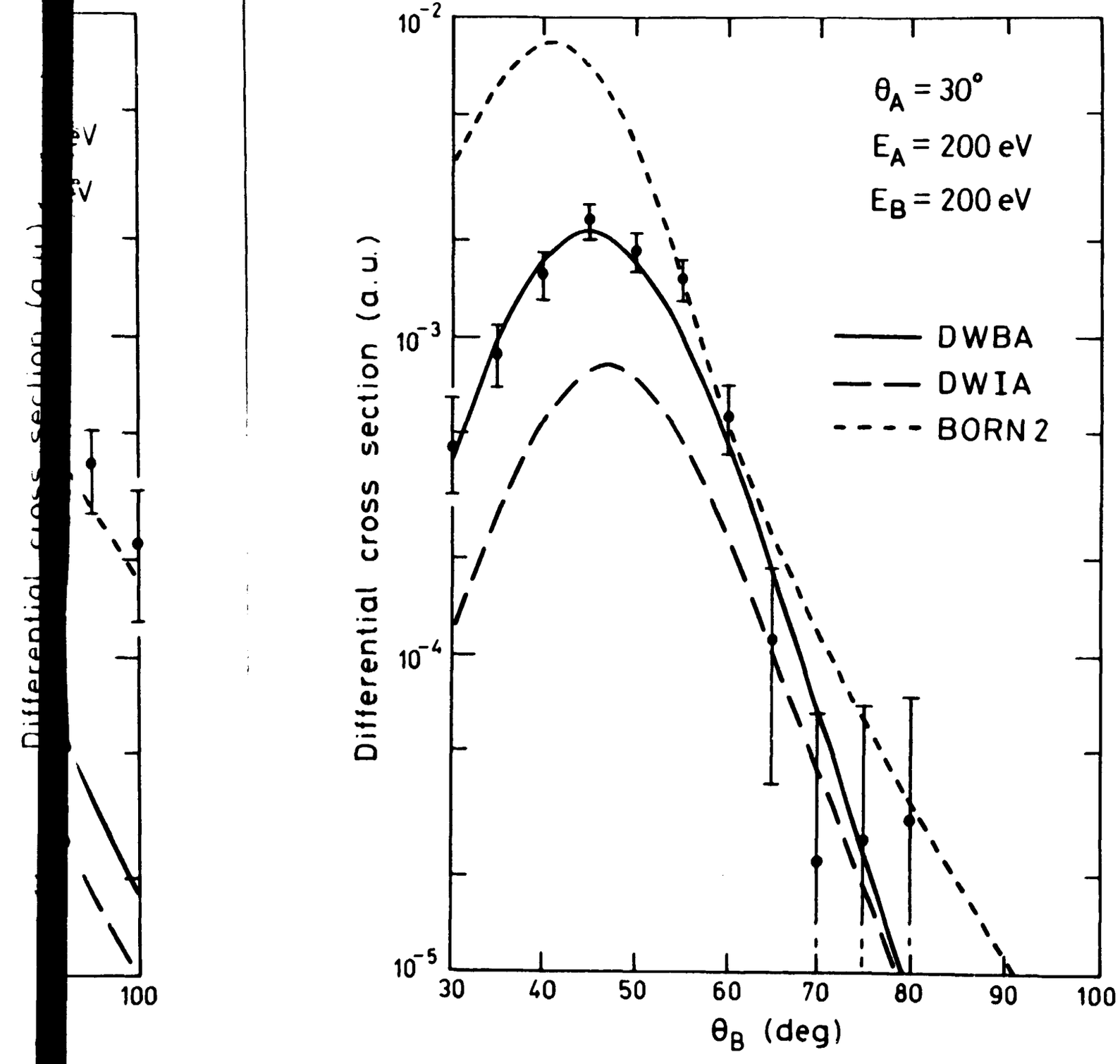
10^{-2}
10^{-3}
10^{-4}
10^{-5}
Differential cross section (a.u.)
$\theta_A = 30°$
$E_A = 200$ eV
$E_B = 200$ eV
DWBA
DWIA
BORN 2
30
40
50
60
70
80
90
100
θ_B (deg)

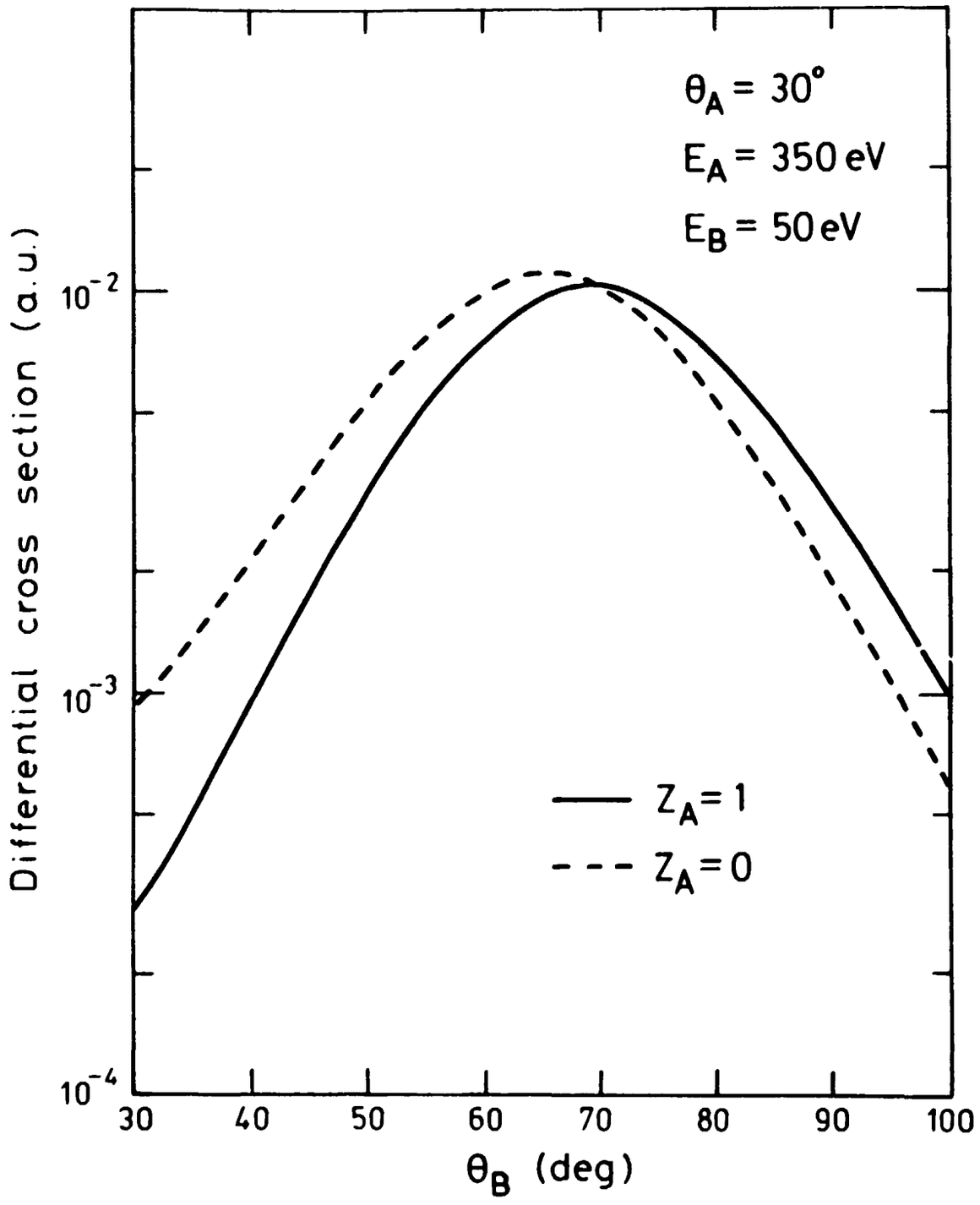
$\theta_A = 30°$
$E_A = 350\,eV$
$E_B = 50\,eV$
$Z_A = 1$
$Z_A = 0$
Differential cross section (a.u.)
10^{-2}
10^{-3}
10^{-4}
30
40
50
60
70
80
90
100
θ_B (deg)